Published in final edited form as:

Nat Microbiol. 2019 July ; 4(7): 1120–1128. doi:10.1038/s41564-019-0416-7.

Viral complementation of immunodeficiency confers protection against enteric pathogens via IFN-λ

Harshad Ingle[1,†], **Sanghyun Lee**[2,†], **Teresa Ai**[1], **Anthony Orvedahl**[3], **Rachel Rodgers**[3], **Guoyan Zhao**[2], **Meagan Sullender**[1], **Stefan T. Peterson**[1], **Marissa Locke**[2], **Ta-Chiang Liu**[2], **Christine C. Yokoyama**[2], **Bridgett Sharp**[5], **Stacey Schultz-Cherry**[5], **Jonathan J. Miner**[1,2,4], and **Megan T. Baldridge**[1,4,*]

[1]Department of Medicine, Washington University School of Medicine, Saint Louis, MO 63110

[2]Department of Pathology and Immunology, Washington University School of Medicine, Saint Louis, MO 63110

[3]Department of Pediatrics, Washington University School of Medicine, Saint Louis, MO 63110

[4]Department of Molecular Microbiology, Washington University School of Medicine, Saint Louis, MO 63110

[5]Department of Infectious Diseases, St. Jude Children's Research Hospital, Memphis, TN 38105

Abstract

Commensal microbes profoundly impact host immunity to enteric viral infections[1]. We have shown that the bacterial microbiota and host antiviral cytokine interferon-lambda (IFN-λ) determine the persistence of murine norovirus in the gut[2,3]. However, the effects of the virome in modulating enteric infections remain unexplored. Here we report that murine astrovirus can complement primary immunodeficiency to protect against murine norovirus and rotavirus infections. Protection against infection was horizontally transferable between immunocompromised mouse strains by cohousing and fecal transplantation. Furthermore, protection against enteric pathogens corresponded with the presence of a specific strain of murine astrovirus in the gut, and this complementation of immunodeficiency required IFN-λ signaling in

*Correspondence to mbaldridge@wustl.edu.

Author contributions: H.I., S.L., T.A., M.S., S.T.P., M.L., T.L., C.C.Y. and M.T.B. performed the experiments. H.I., S.L., T.A., A.O., G.Z., M.S., S.T.P., M.L., T.L., C.C.Y., B.S., R.R., S.S-C, J.J.M. and M.T.B analyzed the results. H.I., S.L., S.S-C., J.J.M and M.T.B designed the project. H.I., S.L. and M.T.B. wrote the manuscript. All authors read and edited the manuscript.

†These authors contributed equally to this work.

Competing interests: C.C.Y and G.Z. hold a patent for detection of murine astrovirus. The authors declare no additional conflicts of interest.

Code availability: The code used for constructing the phylogenetic tree is deposited online on GitHub (https://github.com/RachelRodgers/STL5-phylogenetics).

Data and materials availability: The data from this study are tabulated in the main paper and supplementary materials. All reagents are available from M.T.B. under a material transfer agreement with Washington University. Sequencing data have been uploaded to the European Nucleotide Archive with accession number PRJEB31115.

Supplementary Information:
Supplementary Figures 1–8.

gut epithelial cells. Our study demonstrates that elements of the virome can protect against enteric pathogens in an immunodeficient host.

One Sentence Summary:

Immunodeficiency complemented by virus and IFN-λ

Environmental factors, including commensal bacteria and viruses, affect host susceptibility to genetic diseases and pathogenic infections[4,5]. Both commensal microbes and pathogens can stimulate prolonged systemic activation of innate immunity in immunocompetent animal hosts and confer protection against unrelated pathogens. The introduction of a "wild" mouse microbiota to laboratory mice promotes maturation of the immune system and improves disease resistance[6,7]. Vaccination with Bacillus Calmette-Guérin (BCG), a live-attenuated strain of *Mycobacterium bovis*, promotes systemic lifelong macrophage activation via epigenetic modification of monocytes and hematopoietic stem cells in mice[8–10]. Latent γ-herpesvirus infection enhances interferon-gamma production and systemic macrophage activation, resulting in resistance to lethal bacterial challenge[11]. β-herpesvirus infection induces immunological memory of natural killer (NK) cells in lymphoid and non-lymphoid organs[12]. Host-protozoan interactions in the intestine also influence protection against pathogens, as *Tritrichomonas musculis* activates the epithelial inflammasome to protect against bacterial infection[13].

Here we report the serendipitous discovery of gut-specific protection against two major enteric viral pathogens, norovirus and rotavirus, in immunodeficient mice. This protection was mediated by viral complementation of adaptive immunodeficiency via elevation of type III IFN (IFN-λ) immune responses in the gut.

To test the contribution of innate and adaptive immune cells to regulation of enteric viruses, we orally inoculated wild-type (WT) C57Bl/6J or immunodeficient *Rag1*$^{-/-}$ and *Rag2*$^{-/-}$*Il2rg*$^{-/-}$ mouse strains with persistent enteric murine norovirus strain MNoV^{CR6}, a model pathogen for human norovirus infection[14,15]. Mutations in *Rag1* and *Rag2* render mice deficient in B and T cells[16,17], and mutation of *Il2rg* is associated with reduced lymphocytes and an absence of NK cells, innate lymphoid cells, and gut-associated lymphoid tissue[18]. Consistent with previous studies[2,3], WT and *Rag1*$^{-/-}$ mice exhibited robust viral shedding in stool and readily detectable viral levels in the colon at a persistent timepoint of 14 days post-infection (dpi) (Fig. 1a,b). However, *Rag2*$^{-/-}$*Il2rg*$^{-/-}$ mice exhibited undetectable levels of viral genomes in stool and colon at 14 dpi (Fig. 1a,b). In contrast, *Rag2*$^{-/-}$*Il2rg*$^{-/-}$ mice could be infected with acute systemic MNoV strain MNoV^{CW3}, but failed to clear infection by 14 dpi, consistent with a dependence on adaptive immunity to control this viral strain[19,20] (Fig. 1c). We observed similar protection against MNoV^{CR6} infection in *Il2rg*$^{-/-}$ mice (Supplementary Fig. 1a,b) and in non-obese diabetic (NOD)-*scid Il2rg*$^{-/-}$ (NSG) mice, a widely-used severely immunodeficient strain, compared to NOD controls (Supplementary Fig. 1c,d), suggesting antiviral protection common to multiple immunodeficient mouse strains. We assessed whether this phenomenon was specific to MNoV^{CR6} by inoculating WT and *Rag2*$^{-/-}$*Il2rg*$^{-/-}$ mice with murine rotavirus strain EC (RV^{EC}). WT mice were susceptible to RV^{EC} at early timepoints and cleared

infection by 7 dpi consistent with prior reports[21] (Fig. 1d). In contrast, *Rag2*$^{-/-}$*Il2rg*$^{-/-}$ mice were fully protected against RV^{EC} (Fig. 1d). Collectively, these data suggested an antiviral protective mechanism in severely immunodeficient mice to restrict multiple enteric viruses.

Because the intestinal microbiota regulates both MNoV^{CR6} and RV^{EC} [2,22], and the composition of the intestinal microbiota can be altered in immunodeficient animals[23,24], we speculated that restriction of enteric viral infection could be secondary to an altered microbiota in *Rag2*$^{-/-}$*Il2rg*$^{-/-}$ mice. Thus, we tested whether MNoV^{CR6} susceptibility or restriction was transmissible. Cohousing of MNoV^{CR6}-susceptible WT mice with MNoV^{CR6}-resistant *Rag2*$^{-/-}$*Il2rg*$^{-/-}$ mice for seven days failed to confer resistance to MNoV^{CR6} to WT mice (Fig. 2a). However, when MNoV^{CR6}-susceptible *Rag1*$^{-/-}$ mice were cohoused with *Rag2*$^{-/-}$*Il2rg*$^{-/-}$ mice, *Rag1*$^{-/-}$ mice developed protection against MNoV^{CR6} (Fig. 2b). We considered the hypothesis that a dysbiotic bacterial community may contribute to protection, and tested this by treating *Rag2*$^{-/-}$*Il2rg*$^{-/-}$ mice with antibiotics to deplete the microbiota, followed by fecal transplant (FT) of the microbiota from naïve WT mice into the treated *Rag2*$^{-/-}$*Il2rg*$^{-/-}$ mice 7 days prior to infection with MNoV^{CR6}. Replacement of the fecal microbiota with that of an MNoV^{CR6}-susceptible mouse had no effect on the MNoV^{CR6}-protection in *Rag2*$^{-/-}$*Il2rg*$^{-/-}$ mice (Fig. 2c). We next tested if FT was sufficient to transfer protection against MNoV^{CR6}. We found that FT from *Rag2*$^{-/-}$*Il2rg*$^{-/-}$ donors transplanted to *Rag1*$^{-/-}$, but not WT, recipients protected them from MNoV^{CR6} infection (Fig. 2d). Because FT is a complex mixture of microbes including eukaryotes, bacteria and viruses[5,25], we removed bacteria and eukaryotes by passing the *Rag2*$^{-/-}$*Il2rg*$^{-/-}$ fecal material through a 0.22μm filter. Intriguingly, filtered fecal transplantation (FFT) was sufficient to protect *Rag1*$^{-/-}$ recipients from MNoV^{CR6} (Fig. 2d). The transferable factor(s) conferring protection was thus smaller than 0.22μm, consistent with a virus, secreted vesicle, protein or metabolite. Although the microbiome of cohoused *Rag1*$^{-/-}$ mice showed a shift towards *Rag2*$^{-/-}$*Il2rg*$^{-/-}$ mice, treatment with FFT did not alter bacterial communities in *Rag1*$^{-/-}$ mice, suggesting that MNoV^{CR6}-protection did not depend on alterations to recipient commensal bacteria (Supplementary Fig. 2a,b). Further, we observed protection against MNoV^{CR6} in immunocompetent germ-free mice administered FFT from *Rag2*$^{-/-}$*Il2rg*$^{-/-}$ mice, but not FFT from WT or *Rag1*$^{-/-}$ mice, indicating that this factor mediated protection even in recipient mice lacking a microbiota (Fig. 2e). We further characterized the properties of this factor and found it was sensitive to heat-killing (HK), proteinase K (Prot-K) treatment, and ultraviolet light-irradiation (UV), failing to confer MNoV^{CR6}-protection to *Rag1*$^{-/-}$ recipients after these treatments (Fig. 2f). To determine the durability of the factor in conferring protection, we performed FFT from *Rag2*$^{-/-}$*Il2rg*$^{-/-}$ into *Rag1*$^{-/-}$ mice, and at 7 days post-primary FFT, performed a secondary FFT from these *Rag1*$^{-/-}$ mice into a new cohort of untreated *Rag1*$^{-/-}$ mice, which we infected with MNoV^{CR6} 7 days later (Supplementary Fig. 2c). Even after passaging through a primary recipient, the factor still conferred MNoV^{CR6} protection (Fig. 2g) (Supplementary Fig. 2d). These results in sum were consistent with a heat-, proteinase- and UV-sensitive factor smaller than 0.22μm that can be transmitted to both primary and secondary hosts and which does not modify the recipient microbiota. Overall, these data suggested a viral factor conferring antiviral protection in immunodeficient mice.

We next sought to identify viral factors that could be regulating enteric viral infection. We performed shotgun sequencing on DNA and RNA libraries from *Rag2*$^{-/-}$*Il2rg*$^{-/-}$, WT and *Rag1*$^{-/-}$ FFT material, and analyzed resulting data with VirusSeeker[26]. While the DNA libraries were similar between *Rag2*$^{-/-}$*Il2rg*$^{-/-}$ and controls (Supplementary Fig. 3a), murine astrovirus (muAstV) was identified as the predominant RNA virus only in *Rag2*$^{-/-}$*Il2rg*$^{-/-}$ and *Rag1*$^{-/-}$ mice (Fig. 3a). We further characterized the muAstV reads from these samples, and found that though *Rag1*$^{-/-}$ mice were colonized with a viral strain similar to previously described STL1[27], *Rag2*$^{-/-}$*Il2rg*$^{-/-}$ mice were colonized with two distinct strains, one similar to STL1 and one novel strain, which we designated STL5 (Fig. 3b). Phylogenetic analysis of the STL5 contig showed higher relatedness with STL1 (Supplementary Fig. 3b). QPCR primers specific to conserved sequences of muAstV detected viral genomes in both *Rag2*$^{-/-}$*Il2rg*$^{-/-}$ and *Rag1*$^{-/-}$ mice, while STL5-specific qPCR primers detected muAstV genome copies only in *Rag2*$^{-/-}$*Il2rg*$^{-/-}$ mice (Fig. 3c) (Supplementary Fig. 3c). In addition, STL5 was detected in *Rag1*$^{-/-}$ mice after FFT (Fig. 3c). Similarly, we detected significant levels of STL5 shedding in germ-free mice treated with FFT from *Rag2*$^{-/-}$*Il2rg*$^{-/-}$ mice (Fig. 3d) (Supplementary Fig. 3d). To functionally test whether muAstV was the protective factor, we incubated *Rag2*$^{-/-}$*Il2rg*$^{-/-}$ FFT with a mixture of polyclonal antibodies generated against broadly-conserved muAstV capsid peptides prior to transplantation into *Rag1*$^{-/-}$ mice, which prevented transfer of STL5 but did not affect overall muAstV levels (Supplementary Fig. 3e,f). Prevention of STL5 transfer was associated with a failure to protect against MNoV^{CR6} (Fig. 3e). We next tested whether MNoV^{CR6}-protection was reversible in *Rag2*$^{-/-}$*Il2rg*$^{-/-}$ mice. Indeed, STL5 was cleared in *Rag2*$^{-/-}$*Il2rg*$^{-/-}$ mice transplanted with splenocytes from FFT-primed WT mice, resulting in loss of protection against MNoV^{CR6} (Fig. 3f,g) (Supplementary Fig. 4a-e). Transplantation of NK cells alone was insufficient to clear STL5 or reverse protection in *Rag2*$^{-/-}$*Il2rg*$^{-/-}$ mice (Supplementary Fig. 4f-j). Similarly, *Rag2*$^{-/-}$*Il2rg*$^{-/-}$ FFT administered to WT mice depleted of NK cells did not alter MNoV^{CR6} susceptibility (Supplementary Fig. 4k).

To investigate whether STL5 was acquired in our Washington University (WashU) facility, we analyzed fecal material from *Rag2*$^{-/-}$*Il2rg*$^{-/-}$ mice sent from Taconic Biosciences (Taconic) and Jackson Laboratory (Jax) facilities for muAstV and STL5. *Rag2*$^{-/-}$*Il2rg*$^{-/-}$ mice from Jax were muAstV-positive but both Jax and Taconic mice were STL5-free (Supplementary Fig. 5a,b). We found that Taconic *Rag2*$^{-/-}$*Il2rg*$^{-/-}$ mice were MNoV^{CR6}-susceptible and that FFT from WashU *Rag2*$^{-/-}$*Il2rg*$^{-/-}$ mice transferred protection to Taconic *Rag2*$^{-/-}$*Il2rg*$^{-/-}$ mice (Fig. 3h,i) (Supplementary Fig. 5c). Together, these findings suggest that muAstV is a transferable viral factor that can confer protection to immunodeficient mice from enteric viral infection.

Because IFN-λ is critical in controlling persistent MNoV[3,28,29], we hypothesized that IFN-λ signaling may be dysregulated in mouse strains resistant to MNoV^{CR6}. Indeed, expression of IFN-λ (*Ifnl2/3)* was massively elevated in colons and ileums of naïve *Rag2*$^{-/-}$*Il2rg*$^{-/-}$ (Fig. 4a) (Supplementary Fig. 6a) and NSG mice (Supplementary Fig. 6b,c). Interferon stimulated gene (ISG) *Ifit1* was also increased in *Rag2*$^{-/-}$*Il2rg*$^{-/-}$ and *NSG* intestines (Supplementary Fig. 6d-g). This elevated IFN-λ was significantly reduced in WashU *Rag2*$^{-/-}$*Il2rg*$^{-/-}$ mice after transplantation with FFT-primed WT splenocytes as well as in naïve, muAstV-free Taconic *Rag2*$^{-/-}$*Il2rg*$^{-/-}$ mice, indicating a consistent correlation between the presence of

STL5 and IFN-λ induction (Fig. 4b,c) (Supplementary Fig. 6h). We did not observe differences in IFN-λ or *Ifit1* levels at other mucosal surfaces in *Rag2*$^{-/-}$*Il2rg*$^{-/-}$ mice, suggesting a gut-specific phenomenon (Supplementary Fig. 7a,b). We detected higher *Ifnl2/3* expression in the small intestine epithelial fraction compared to the lamina propria, suggesting *Ifnl2/3* was epithelial-derived (Supplementary Fig. 7c). This compartmentalized *Ifnl2/3* expression was associated with similar compartmentalization of STL5, raising the possibility of an epithelial cell niche for this viral strain (Supplementary Fig. 7d,e). Of interest, expression of type I IFNs was unchanged in *Rag2*$^{-/-}$*Il2rg*$^{-/-}$ colons, and type II IFN was decreased (*Ifng*), likely secondary to the absence of T and NK cells (Supplementary Fig. 7f-j). Levels of ISGs *Ifi44* and *Ifit1* in *Rag2*$^{-/-}$*Il2rg*$^{-/-}$ mice were comparable to levels in WT mice treated with 3 μg of IFN-λ, a sufficient IFN-λ dose to cure MNoV^{CR6} in WT mice (Fig. 4d) (Supplementary Fig. 7k)[3,29]. Next, we tested whether transmission of MNoV^{CR6}-protection required IFN-λ. We previously generated *Rag1*$^{-/-}$*Ifnlr1*$^{-/-}$ and *Rag1*$^{-/-}$*Ifnlr1*$^{f/f}$-*Villincre* mice which respectively lack the IFN-λ receptor in all or specifically intestinal epithelial cells[29]. We transferred FFT from *Rag2*$^{-/-}$*Il2rg*$^{-/-}$ to these mice and their littermate controls and found that MNoV^{CR6}-protection transferred to *Rag1*$^{-/-}$*Ifnlr1*$^{+/+}$ (Supplementary Fig. 8a,b) and *Rag1*$^{-/-}$*Ifnlr1*$^{f/f}$ mice (Fig. 4e) (Supplementary Fig. 8c), similar to *Rag1*$^{-/-}$ mice (Fig. 2d). However, protection was not transferred to *Rag1*$^{-/-}$*Ifnlr1*$^{-/-}$ (Supplementary Fig. 8a,b) or *Rag1*$^{-/-}$*Ifnlr1*$^{f/f}$-*Villincre* mice (Fig. 4e) (Supplementary Fig. 8c), indicating that intact IFN-λ signaling was necessary for transmission of MNoV^{CR6}-protection. In both *Rag1*$^{-/-}$ and *Rag1*$^{-/-}$*Ifnlr1*$^{-/-}$ recipients, STL5 levels remain lower than total muAstV levels (Supplementary Fig. 8d,e). Of note, *Rag1*$^{-/-}$*Ifnlr1*$^{f/f}$ recipients were protected against a 10-fold higher MNoV^{CR6} dose, indicating dose-independent protection not transferable to *Rag1*$^{-/-}$*Ifnlr1*$^{f/f}$-*Villincre* mice (Supplementary Fig. 8f). Importantly, elevated IFN-λ and ISG expression in *Rag2*$^{-/-}$*Il2rg*$^{-/-}$ mice or after FFT in *Rag1*$^{-/-}$ mice did not induce intestinal inflammation, evidenced by the lack of inflammatory cell infiltration or tissue damage (Fig. 4f). To further confirm that elevated IFN-λ was responsible for resistance in immunodeficient mice, we generated *Il2rg*$^{-/-}$*Ifnlr1*$^{-/-}$ and *Rag2*$^{-/-}$*Il2rg*$^{-/-}$*Ifnlr1*$^{-/-}$ mice. We observed that abrogation of IFN-λ signaling in *Rag2*$^{-/-}$*Il2rg*$^{-/-}$*Ifnlr1*$^{-/-}$ and *Il2rg*$^{-/-}$*Ifnlr1*$^{-/-}$ mice was sufficient to rescue MNoV^{CR6} infection (Fig. 4g) (Supplementary Fig. 8g). Despite restored MNoV^{CR6} susceptibility, these mice maintained the capacity to transmit protection to *Rag1*$^{-/-}$ mice by FFT, indicating that the loss of MNoV^{CR6}-protection was due to the absence of IFN-λ signaling and not loss of the transferable factor (Fig. 4h) (Supplementary Fig. 8g,h). In sum, these data indicate that induction of IFN-λ-dependent immunity by muAstV confers protection against MNoV in immunodeficient mice.

In this study, we discovered that chronic muAstV complements defects in adaptive immunity by elevating cell-intrinsic IFN-λ in the intestinal epithelial barrier in immunodeficient mice. *Rag2*$^{-/-}$*Il2rg*$^{-/-}$ and NSG mice are two of the most commonly used immunodeficient strains for transplantation and humanized mouse models[30]. This study demonstrated the potential for these lines to harbor chronic viral infections, resulting in immunologically distinct baseline IFN responses, which might alter experimental outcomes. We suspect that other immunodeficient models could also be affected by virus-mediated altered IFN-λ responses. These differential baselines in intestinal innate immunity should be carefully considered for

transplantation studies using immunodeficient mouse models. Since we observed heightened intestine-specific IFN-λ in multiple genetically distinct immunodeficient mouse models, we hypothesize that regulation of IFN-λ-driven responses in these normally vulnerable mice may be a common mechanism to enhance innate resistance to pathogens. Furthermore, our discovery that type I and II IFNs were not elevated indicates a specific and compartmentalized IFN-λ response at the mucosal barrier that did not cause any observable adverse effects to the mice. Thus, an element of the enteric virome can confer innate immune-mediated protection of an immunodeficient host without triggering adverse systemic inflammation.

Methods

Mice:

Wild-type (WT) C57BL/6J (stock no. 000664), *Rag1*$^{-/-}$ (B6.129S7-*Rag1*^{tm1Mom}*/J*, stock no. 002216), *Il2rg*$^{-/-}$ (B6.129S4-*Il2rg*^{tm1Wjl}*/J*, catalog no. 003174), NOD (NOD/ShiLtJ, Non-obese Diabetic, stock no. 001976), and NSG (NOD.Cg-*Prkdc*^{scid}*Il2rg*^{tm1Wjl}*/SzJ*, stock no. 005557) mice were purchased from Jackson Laboratories (Bar Harbor, ME) and maintained at Washington University School of Medicine under specific-pathogen-free conditions according to University guidelines. *Rag2*$^{-/-}$*Il2rg*$^{-/-}$ were generated by crossing of *Il2rg*$^{-/-}$ (B6.129S4-*Il2rg*^{tm1Wjl}*/J*, catalog no. 003174) mice from Jackson Laboratories with *Rag2*$^{-/-}$ (B6.129S6-*Rag2*^{tm1Fwa} *N12*, catalog no. RAGN12) mice from Taconic (Rensselaer, NY). Stools from *Rag2*$^{-/-}$*Il2rg*$^{-/-}$ mice shipped from Taconic Biosciences (B6-*Rag2*^{tm1Fwa} *Il2rg*^{tm1Wjl}) and Jackson Laboratory (C;129S4-*Rag2*$^{tm1.1Flv}$ *Il2rg*$^{tm1.1Flv}$/J, stock no. 014593) facilities were used for analyses, and *Rag2*$^{-/-}$*Il2rg*$^{-/-}$ mice from Taconic were used directly for experiments upon arrival at Washington University facilities. Germ-free Swiss Webster mice were purchased from Taconic Biosciences and maintained in sterile, flexible-film plastic gnotobiotic isolators at the Washington University School of Medicine Central Gnotobiotic Facility. Generation of *Ifnlr1*$^{-/-}$, *Ifnlr1*$^{f/f}$, and *Ifnlr1*$^{f/f}$-*Villincre* (*Ifnlr1*$^{tm1a(EUCOMM)Wtsi}$) mice was previously described, as was generation of *Rag1*$^{-/-}$*Ifnlr1*$^{-/-}$, *Rag1*$^{-/-}$*Ifnlr1*$^{f/f}$, and *Rag1*$^{-/-}$*Ifnlr1*$^{f/f}$-*Villincre* mice[29]. For generation of *Rag2*$^{-/-}$*Il2rg*$^{-/-}$*Ifnlr1*$^{-/-}$ knockout mice, *Rag2*$^{-/-}$*Il2rg*$^{-/-}$ mice described above were crossed with *Ifnlr1*$^{-/-}$ mice. Equal ratios of adult male and female mice, aged 6 to 12 weeks, were used in all experiments for all strains, with the exclusion of cohousing experiments described below. Experimental mice were cohoused with up to 5 mice of the same sex per cage with autoclaved standard chow pellets and water provided *ad libitum*.

Virus generation and infections:

MNoV stocks for MNoV^{CR6} (CR6) and MNoV^{CW3} (CW3) were generated from molecular clones as previously described[31,32]. Briefly, plasmids encoding the MNoV genome were transfected into 293T cells to generate infectious virus, which was subsequently passaged on BV2 cells. After two passages, BV2 cultures were frozen and thawed to liberate virions. Then, cultures were cleared of cellular debris and concentrated by ultracentrifugation. Titers of virus stocks were determined by plaque assay on BV2 cells as described[32]. For MNoV infections, conventional specific-pathogen free and germ-free mice were inoculated with a dose of 10^6 pfu of the indicated viral strain, except as otherwise mentioned. Germ-free mice

were infected with a dose of 10^7 pfu of the indicated viral strain. All mice were infected at 6 to 8 weeks of age by the oral route in a volume of 25 µl. Mouse rotavirus (RV) strain EC (RV^{EC}) was provided by Mary Estes (Baylor College of Medicine)[33]. Mice received 10^5 50% shedding doses (SD50) of RV in 100µl, preceded by 100µl 1.33% (w/v) sodium bicarbonate (Sigma-Aldrich) by oral gavage. For all experiments, stool and tissues were harvested from mice into 2-ml tubes (Sarstedt, Germany) with 1-mm diameter zirconia/silica beads (Biospec, Bartlesville, OK). Tissues were frozen on dry ice and either processed on the same day or stored at −80°C.

Cohousing and fecal transplants:

For cohousing experiments, female mice of different genotypes were cohoused in a 1:1 ratio for 7 days, then separated by genotype prior to further treatment or infection. For fecal transplantation, stool pellets were collected and resuspended in sterile PBS to a final concentration of 200 mg/ml by weight. 25µl of this material was orally administered to mice on two consecutive days, as previously described[34]. For filtered fecal transplantation, the resuspended fecal material was filtered using a 0.22µm syringe filter (Millipore). 25µl of the filtrate was orally administered to mice on two consecutive days. Mice were also orally administered for two consecutive days with filtrate incubated at 95°C for 10 minutes for heat inactivation, treated with 1mg/ml of Proteinase K for enzymatic digestion at 56°C for 15 minutes, or treated with 254nm UV light in a Biosafety laminar airflow hood for 60 minutes for UV inactivation.

Splenocyte transplantation:

Six- to eight-week-old WT C57BL/6J mice were ‘primed’ by oral inoculation of FFT from naïve *Rag2*$^{-/-}$*Il2rg*$^{-/-}$ mice for 7 days. Spleens were isolated and gently mashed in PBS and filtered through 70 micron cell strainer to get a single cell suspension of splenocytes. 2×10^6 splenocytes were intravenously injected in naïve *Rag2*$^{-/-}$*Il2rg*$^{-/-}$ mice. Fourteen days after transplantation, cells from peripheral blood were isolated and analyzed by flow cytometry.

NK cell transplantation and depletion:

Mouse NK cells were isolated by negative selection of bulk splenocytes from *Rag1*$^{-/-}$ mice using the NK cell isolation kit (Miltenyi Biotec). All cells except mouse NK cells were magnetically labelled and separated using MACS LS columns (Miltenyi Biotec). The purity of isolated NK cells was >90%. 2×10^6 purified NK cells were intravenously injected in naive *Rag2*$^{-/-}$*Il2rg*$^{-/-}$ mice. Fourteen days after transplantation, cells from peripheral blood were analyzed by flow cytometry for NK1.1 positive cells. For NK cell depletion, mice were intraperitoneally injected with 200µg of anti-NK1.1 antibody (Leinco) 2 days prior to FFT treatment and 1 day before $MNoV^{CR6}$ infection. Isotype IgG1 antibody (Bio X Cell) was used as control for depletion.

Small intestinal cell fractionation:

The epithelial and lamina propria fractions were isolated from small intestinal segments as previously described[29]. Briefly, mice were euthanized and small intestinal segments between duodenum and jejunum, and jejunum and ileum were collected separately. Tissues were

washed in ice cold PBS twice, chopped and incubated with stripping buffer (10% fetal bovine serum, 15 mM HEPES, 5 mM EDTA, in 1x HBSS) for 20 min at 37°C followed by vortexing for 15 sec. The dissociated cells were passed through a 100μm and 40μm filter and washed with ice cold PBS. The collected cells comprised the epithelial fraction. The remaining tissue was used as the lamina propria fraction.

Flow cytometry:

Mouse peripheral blood leukocytes were stained with antibodies for 30 minutes in the dark, including fluorescently-conjugated antibodies specific to CD45.2 (BD Biosciences; clone-30-F11), CD3 (Biolegend; clone-145–2C11), B220 (Biolegend; clone-RA3–6B2), CD25 (Biolegend; clone-PC61.5), CD8b (Biolegend; clone-YTS156.7.7), CD4 (Biolegend; clone-GK1.5), and NK1.1 (Biolegend; clone-PK136). Cells were then washed with FACS buffer (PBS, 2% FBS, 2mM EDTA) and resuspended in FACS buffer before performing multicolor flow cytometric analysis using a FACS CantoII machine (BD Biosciences). Flow cytometry data were analyzed using FlowJo software version 10 (Tree Star).

Murine astrovirus antibodies and neutralization assay:

Rabbit polyclonal antibodies were commercially generated by using peptide sequences GEDDEYYTDEEGESDEGAE (from capsid of muAstV strain BSRI; peptide sequence is GEDDEYYTDEEGESDEGAQ for STL5 and GEGEDYSTDEEGESDEGA for STL1), CGGDRNRWPYRNQIE (from capsid of muAstV strain STL1; sequence conserved in STL5) and CSEFLAQRESRGHAE (from capsid of muAstV strain STL1; peptide sequence unknown for STL5). The specificity and concentration of antibody was determined by ELISA using the same peptides. For neutralization experiments, muAstV antibodies were mixed in equal concentrations (25μg each) prior to incubating with FFT for 1h at 37°C. Isotype IgG antibody (Sigma; 75μg total) was incubated with FFT for 1h at 37°C as a control. This mix of FFT and muAstV antibodies or isotype antibody was used for transplantation.

Antibiotic and Interferon-lambda (IFN-λ) treatments:

For antibiotic treatment, cages of mice were treated as previously described[2] with an antibiotic cocktail (VNAM) [1 g/L ampicillin, 1 g/L metronidazole, 1 g/L neomycin, 0.5 g/L vancomycin (Sigma, St. Louis, MO)] in 20 mg/mL grape Kool-Aid (Kraft Foods, Northfield, IL) or with Kool-Aid alone for 2 weeks starting at 6 weeks of age. Recombinant IFN-λ was provided by Bristol-Myers Squibb (Seattle, WA) as a monomeric conjugate comprised of 20-kDa linear polyethylene glycol (PEG) attached to the amino terminus of murine IFN-λ, as previously reported[3]. For treatment of mice, 3μg of IFN-λ diluted in PBS was injected intraperitoneally.

Quantitative reverse transcription PCR (qPCR):

RNA from stool was isolated using a ZR-96 Viral RNA kit (Zymo Research, Irvine, CA). Total RNA from tissues or cells was isolated using Tri Reagent (Invitrogen) and a Direct-zol-96 RNA kit (Zymo Research) according to the manufacturer's protocol. Five μl of RNA from stool or 1 μg of RNA from tissue was used as a template for cDNA synthesis with the

ImPromII reverse transcriptase system (Promega, Madison, WI). DNA contamination was removed using the DNAfree kit (Life Technologies). MNoV qPCR assays were performed, using a standard curve for determination of absolute viral genome copies, as described previously[35]. QPCR for housekeeping gene *Rps29* was performed as previously described[29]. A PrimeTime qPCR assay for *Ifit1* (Mm.PT.58.32674307), *Ifi44* (Mm.PT.58.12162024), *Ifna1* (Mm.PT.58.43426930.g), *Ifna4* (Mm.PT.58.7678281.g), *Ifna11* (Mm.PT.58.43054322.g), *Ifnb1* (Mm.PT.58.30132453.g), *Ifng* (Mm.PT.58.30096391) (Integrated DNA Technologies) and a Taqman assay for *Ifnl2/3* (Mm04204156_gH) (Thermo Fisher Scientific) were performed using the same protocol. QPCR for murine astrovirus (muAstV), designed to detect all muAstV strains using primers against conserved regions, was performed as described previously[27]. A SYBR green qPCR assay was performed for muAstV STL5 using Power SYBR green master mix (Applied Biosystems) and specific primers (5'-CTTATCAGAATGCGGCCTAC-3', 5'-TGAGTGCACTTTCACAGTAC-3'). Rotavirus genome copies were detected using *NSP3* specific primer pairs (5'-CTTCTGGACTACGACAGACTATTT-3', 5'-GATGTTTGATCGGTTCGTTGTG-3') with a (5'-AGCGCTGCAACTTAGACTACGCAT-3') 5′ 6-carboxyfluorescein (FAM) dye label, 3′ nonfluorescent quencher (NFQ), and minor groove binder (MGB).

Sequencing library preparation and analysis:

DNA and cDNA libraries were prepared as described previously[36]. Briefly, DNA was extracted using phenol-chloroform extraction followed by purification using the DNeasy Blood and Tissue Kit (Qiagen) and cDNA was prepared from total RNA isolated from filtered fecal material as described above. Both DNA and cDNA were used for tagmentation using the Nextera DNA Library Preparation kit (Illumina). This was followed by PCR mediated adapter ligation using KAPA HiFi PCR master mix (Roche). The tagmented and indexed cDNA library was selected for approx. 200bp size using AMPure XP magnetic beads. Equimolar quantities of libraries were run on the Illumina NextSeq platform using a paired end 2×150 protocol. VirusSeeker-Discovery[26] was used to assemble sequences into contigs and to detect contigs sharing nucleotide and protein level sequence similarity to known viruses. Briefly, sequences were adapter-trimmed, quality controlled, and dereplicated. Host sequences were filtered by aligning sequences to mouse reference genome using BWA-MEM[37]. For each sample, CD-HIT[38] was used to dereplicate sequences at 95% identity over 95% overlap of the length. The longest sequence from each cluster and the top three sequences were taken as representatives and used for *de novo* assembly using Newbler v2.8 (454 Life Sciences, USA) and Phrap (http://www.phrap.org/) in a two-step assembly. Potential unique viral contigs and reads were sequentially queried against the NCBI NT/NR databases, and only sequences matching exclusively to viral sequences were kept for further analysis. All sequences aligning to viruses were further classified into viral families based on the NCBI taxonomic identity of the best hit.

16S rDNA sequencing and analysis:

DNA extracted from fecal pellets using phenol:chloroform was used for 16S rDNA sequencing. Primer selection and PCRs were performed as described previously[39]. Briefly, each sample was amplified in triplicate with Golay-barcoded primers specific for the V4 region (F515/R806), combined, and confirmed by gel electrophoresis. Genomic DNA was

amplified by PCR using Platinum High Fidelity Taq (Invitrogen) as described previously[2]. Amplicons were pooled and purified with 0.6x Agencourt Ampure XP beads (Beckman-Coulter) according to the manufacturer's instructions. The final pooled samples, along with aliquots of the three sequencing primers, were sent to the DNA Sequencing Innovation Lab (Washington University School of Medicine) for sequencing by the 2×250bp protocol with the Illumina MiSeq platform. 16S sequence analysis was performed using QIIME (Quantitative Insights Into Microbial Ecology, version 1.8.0)[40]. Raw sequence fastq files were quality filtered and demultiplexed with the following criteria: the maximum number of consecutive low quality base calls allowed was 3, the minimum number of consecutive high quality base calls must be greater than 75% of the input sequence length, the PHRED quality threshold was set to 19, and reverse-complement mapping barcodes were used. Closed reference operational taxonomic units (OTUs) sharing 97% identity were clustered with the UCLUST algorithm[41] and assigned taxonomy according to the Greengenes database (version 13.8)[42]. Unweighted unifrac distance matrices were computed and 3-dimensional principal coordinates analysis plots were generated with Emperor[43].

Phylogenetic analysis:

ORF2 protein sequences for the astrovirus strains of interest were downloaded from NCBI GenBank Release 226.0[44]. The nucleotide sequence for the STL5 ORF2 contig was translated with EMBOSS Transeq[45]. Sequences were aligned with Clustal X v.2.1 using default parameters[46]. Maximum likelihood phylogenetic analysis was performed with the RAxML v.8.2.12 rapid bootstrap method ("-f a" option) with 1,000 bootstrap replicates using the GAMMA model of rate heterogeneity and ML estimate of the alpha parameter with the BLOSUM62 substitution matrix[47].

Histology:

Ileums and colons were harvested, and intestinal contents were flushed with PBS followed by 10% neutral buffered formalin. Tissues were cut longitudinally, pinned overnight in 10% neutral buffered formalin, washed three times with 70% ethanol, blocked in 2% Agar (Sigma Aldrich), and embedded in paraffin for sectioning. All sections were cut and mounted at the Washington University Pulmonary Morphology core facility. Brightfield images were acquired at 20X magnification with an Olympus BX51 microscope equipped with UPlanFL 10X/0.30, 20X/0.50, 40X/0.75, and 100X/1.30 Oil Iris objective lenses, an Olympus DP70 or DP22 camera and DP Controller or cellSens Standard v1.17 software.

Statistical Analysis:

Data were analyzed with Prism 7 software (GraphPad Software, San Diego, CA). In all graphs, three asterisks indicate $P<0.001$, two asterisks indicate $P<0.01$, one asterisk indicates $P<0.05$, and ns indicates not significant ($P>0.05$) as determined by unpaired nonparametric Mann-Whitney test when comparing two groups or nonparametric Kruskal-Wallis test with Dunn's multiple comparison when comparing three or more groups as designated in figure legends. Sample category 16S results were compared using PERMANOVA in QIIME with 999 permutations.

Supplementary Material

Refer to Web version on PubMed Central for supplementary material.

Acknowledgments:

We acknowledge all members of the Baldridge lab for helpful discussions. We also thank J. Hoisington-Lopez for assistance with sequencing, D. Kreamalmeyer for animal care and breeding, the Washington University Pulmonary Morphology core facility for assistance with histology, and J. White and the Washington University Central Gnotobiotic Facility for assistance with germ-free mice. We are grateful to the Estes lab for providing murine rotavirus.

Funding: H.I. was supported by the Children's Discovery Institute of Washington University and St. Louis Children's Hospital Postdoctoral Research grant (MI-F-2018–712). S.L. was supported by the Basic Science Research Program through the National Research Foundation of Korea funded by the Ministry of Education (NRF-2016R1A6A3A03012352). A.O. was funded by the Pediatric Infectious Diseases Society/ St. Jude Children's Research Hospital Fellowship Program in Basic Research and NIH training grant T32AI106688. C.C.Y. was supported by NIH training grant T32AI007163. S.S-C was supported by ALSAC and NIH grant R03 AI126101–01. J.J.M. was supported by NIH grant K08 AR07091. M.T.B. was supported by NIH grants K22 AI127846, R01 AI127552, R01 AI139314 and R01 AI141478, Digestive Diseases Research Core Centers P30 DK052574, the Pew Biomedical Scholars Program and the Global Probiotics Council's Young Investigator Grant for Probiotics Research.

References and Notes

1. Pfeiffer JK & Virgin HW Viral immunity. Transkingdom control of viral infection and immunity in the mammalian intestine. Science 351, doi:10.1126/science.aad5872(2016).
2. Baldridge MT et al. Commensal microbes and interferon-lambda determine persistence of enteric murine norovirus infection. Science 347, 266–269, doi:10.1126/science.1258025 (2015). [PubMed: 25431490]
3. Nice TJ et al. Interferon-lambda cures persistent murine norovirus infection in the absence of adaptive immunity. Science 347, 269–273, doi:10.1126/science.1258100 (2015). [PubMed: 25431489]
4. Netea MG et al. Trained immunity: A program of innate immune memory in health and disease. Science 352, aaf1098, doi:10.1126/science.aaf1098 (2016).
5. Virgin HW The virome in mammalian physiology and disease. Cell 157, 142–150, doi:10.1016/j.cell.2014.02.032 (2014). [PubMed: 24679532]
6. Rosshart SP et al. Wild Mouse Gut Microbiota Promotes Host Fitness and Improves Disease Resistance. Cell 171, 1015–1028 e1013, doi:10.1016/j.cell.2017.09.016 (2017). [PubMed: 29056339]
7. Beura LK et al. Normalizing the environment recapitulates adult human immune traits in laboratory mice. Nature 532, 512–516, doi:10.1038/nature17655 (2016). [PubMed: 27096360]
8. Kaufmann E et al. BCG Educates Hematopoietic Stem Cells to Generate Protective Innate Immunity against Tuberculosis. Cell 172, 176–190 e119, doi:10.1016/j.cell.2017.12.031 (2018). [PubMed: 29328912]
9. Kleinnijenhuis J et al. Bacille Calmette-Guerin induces NOD2-dependent nonspecific protection from reinfection via epigenetic reprogramming of monocytes. Proc Natl Acad Sci U S A 109, 17537–17542, doi:10.1073/pnas.1202870109 (2012). [PubMed: 22988082]
10. Arts RJW et al. BCG Vaccination Protects against Experimental Viral Infection in Humans through the Induction of Cytokines Associated with Trained Immunity. Cell Host Microbe 23, 89–100 e105, doi:10.1016/j.chom.2017.12.010 (2018). [PubMed: 29324233]
11. Barton ES et al. Herpesvirus latency confers symbiotic protection from bacterial infection. Nature 447, 326–329, doi:10.1038/nature05762 (2007). [PubMed: 17507983]
12. Sun JC, Beilke JN & Lanier LL Adaptive immune features of natural killer cells. Nature 457, 557–561, doi:10.1038/nature07665 (2009). [PubMed: 19136945]

13. Chudnovskiy A et al. Host-Protozoan Interactions Protect from Mucosal Infections through Activation of the Inflammasome. Cell 167, 444–456 e414, doi:10.1016/j.cell.2016.08.076 (2016). [PubMed: 27716507]
14. Nice TJ, Strong DW, McCune BT, Pohl CS & Virgin HW A single-amino-acid change in murine norovirus NS1/2 is sufficient for colonic tropism and persistence. J Virol 87, 327–334, doi: 10.1128/JVI.01864-12 (2013). [PubMed: 23077309]
15. Thackray LB et al. Murine noroviruses comprising a single genogroup exhibit biological diversity despite limited sequence divergence. Journal of virology 81, 10460–10473, doi:10.1128/JVI. 00783-07 (2007). [PubMed: 17652401]
16. Mombaerts P et al. RAG-1-deficient mice have no mature B and T lymphocytes. Cell 68, 869–877 (1992). [PubMed: 1547488]
17. Shinkai Y et al. RAG-2-deficient mice lack mature lymphocytes owing to inability to initiate V(D)J rearrangement. Cell 68, 855–867 (1992). [PubMed: 1547487]
18. Cao X et al. Defective lymphoid development in mice lacking expression of the common cytokine receptor gamma chain. Immunity 2, 223–238 (1995). [PubMed: 7697543]
19. Chachu KA, LoBue AD, Strong DW, Baric RS & Virgin HW Immune mechanisms responsible for vaccination against and clearance of mucosal and lymphatic norovirus infection. PLoS Pathog 4, e1000236, doi:10.1371/journal.ppat.1000236 (2008). [PubMed: 19079577]
20. Chachu KA et al. Antibody is critical for the clearance of murine norovirus infection. J Virol 82, 6610–6617, doi:10.1128/JVI.00141-08 (2008). [PubMed: 18417579]
21. Zhang B et al. Viral infection. Prevention and cure of rotavirus infection via TLR5/NLRC4-mediated production of IL-22 and IL-18. Science 346, 861–865, doi:10.1126/science.1256999 (2014). [PubMed: 25395539]
22. Uchiyama R, Chassaing B, Zhang B & Gewirtz AT Antibiotic treatment suppresses rotavirus infection and enhances specific humoral immunity. J Infect Dis 210, 171–182, doi:10.1093/infdis/jiu037 (2014). [PubMed: 24436449]
23. Galvez EJC, Iljazovic A, Gronow A, Flavell R & Strowig T Shaping of Intestinal Microbiota in Nlrp6- and Rag2-Deficient Mice Depends on Community Structure. Cell reports 21, 3914–3926, doi:10.1016/j.celrep.2017.12.027 (2017). [PubMed: 29281837]
24. Handley SA et al. SIV Infection-Mediated Changes in Gastrointestinal Bacterial Microbiome and Virome Are Associated with Immunodeficiency and Prevented by Vaccination. Cell Host Microbe 19, 323–335, doi:10.1016/j.chom.2016.02.010 (2016). [PubMed: 26962943]
25. Norman JM, Handley SA & Virgin HW Kingdom-agnostic metagenomics and the importance of complete characterization of enteric microbial communities. Gastroenterology 146, 1459–1469, doi:10.1053/j.gastro.2014.02.001 (2014). [PubMed: 24508599]
26. Zhao G et al. VirusSeeker, a computational pipeline for virus discovery and virome composition analysis. Virology 503, 21–30, doi:10.1016/j.virol.2017.01.005 (2017). [PubMed: 28110145]
27. Yokoyama CC et al. Adaptive immunity restricts replication of novel murine astroviruses. J Virol 86, 12262–12270, doi:10.1128/JVI.02018-12 (2012). [PubMed: 22951832]
28. Lee S et al. Norovirus Cell Tropism Is Determined by Combinatorial Action of a Viral Non-structural Protein and Host Cytokine. Cell Host Microbe 22, 449–459 e444, doi:10.1016/j.chom. 2017.08.021 (2017). [PubMed: 28966054]
29. Baldridge MT et al. Expression of Ifnlr1 on intestinal epithelial cells is critical to the antiviral effects of IFN-lambda against norovirus and reovirus. J Virol, doi:10.1128/JVI.02079-16 (2017).
30. Shultz LD, Brehm MA, Garcia-Martinez JV & Greiner DL Humanized mice for immune system investigation: progress, promise and challenges. Nat Rev Immunol 12, 786–798, doi:10.1038/nri3311 (2012). [PubMed: 23059428]
31. Strong DW, Thackray LB, Smith TJ & Virgin HW Protruding domain of capsid protein is necessary and sufficient to determine murine norovirus replication and pathogenesis in vivo. J Virol 86, 2950–2958, doi:10.1128/JVI.07038-11 (2012). [PubMed: 22258242]
32. Orchard RC et al. Discovery of a proteinaceous cellular receptor for a norovirus. Science 353, 933–936, doi:10.1126/science.aaf1220 (2016). [PubMed: 27540007]

33. Feng N, Burns JW, Bracy L & Greenberg HB Comparison of mucosal and systemic humoral immune responses and subsequent protection in mice orally inoculated with a homologous or a heterologous rotavirus. J Virol 68, 7766–7773 (1994). [PubMed: 7966566]
34. Moon C et al. Vertically transmitted faecal IgA levels determine extra-chromosomal phenotypic variation. Nature 521, 90–93, doi:10.1038/nature14139 (2015). [PubMed: 25686606]
35. Baert L et al. Detection of murine norovirus 1 by using plaque assay, transfection assay, and real-time reverse transcription-PCR before and after heat exposure. Applied and environmental microbiology 74, 543–546, doi:10.1128/Aem.01039-07 (2008). [PubMed: 18024676]
36. Baym M et al. Inexpensive multiplexed library preparation for megabase-sized genomes. PLoS One 10, e0128036, doi:10.1371/journal.pone.0128036 (2015). [PubMed: 26000737]
37. Li H & Durbin R Fast and accurate long-read alignment with Burrows-Wheeler transform. Bioinformatics 26, 589–595, doi:10.1093/bioinformatics/btp698 (2010). [PubMed: 20080505]
38. Li W & Godzik A Cd-hit: a fast program for clustering and comparing large sets of protein or nucleotide sequences. Bioinformatics 22, 1658–1659, doi:10.1093/bioinformatics/btl158 (2006). [PubMed: 16731699]
39. Caporaso JG et al. Global patterns of 16S rRNA diversity at a depth of millions of sequences per sample. Proc Natl Acad Sci U S A 108 Suppl 1, 4516–4522, doi:10.1073/pnas.1000080107 (2011). [PubMed: 20534432]
40. Caporaso JG et al. QIIME allows analysis of high-throughput community sequencing data. Nat Methods 7, 335–336, doi:10.1038/nmeth.f.303 (2010). [PubMed: 20383131]
41. Edgar RC Search and clustering orders of magnitude faster than BLAST. Bioinformatics 26, 2460–2461, doi:10.1093/bioinformatics/btq461 (2010). [PubMed: 20709691]
42. McDonald D et al. An improved Greengenes taxonomy with explicit ranks for ecological and evolutionary analyses of bacteria and archaea. ISME J 6, 610–618, doi:10.1038/ismej.2011.139 (2012). [PubMed: 22134646]
43. Vazquez-Baeza Y, Pirrung M, Gonzalez A & Knight R EMPeror: a tool for visualizing high-throughput microbial community data. Gigascience 2, 16, doi:10.1186/2047-217X-2-16 (2013). [PubMed: 24280061]
44. Clark K, Karsch-Mizrachi I, Lipman DJ, Ostell J & Sayers EW GenBank. Nucleic Acids Res 44, D67–72, doi:10.1093/nar/gkv1276 (2016). [PubMed: 26590407]
45. Rice P, Longden I & Bleasby A EMBOSS: the European Molecular Biology Open Software Suite. Trends Genet 16, 276–277 (2000). [PubMed: 10827456]
46. Larkin MA et al. Clustal W and Clustal X version 2.0. Bioinformatics. 23, 2947–2948 (2007). [PubMed: 17846036]
47. Stamatakis A RAxML version 8: a tool for phylogenetic analysis and post-analysis of large phylogenies. Bioinformatics 30, 1312–1313, doi:10.1093/bioinformatics/btu033 (2014). [PubMed: 24451623]

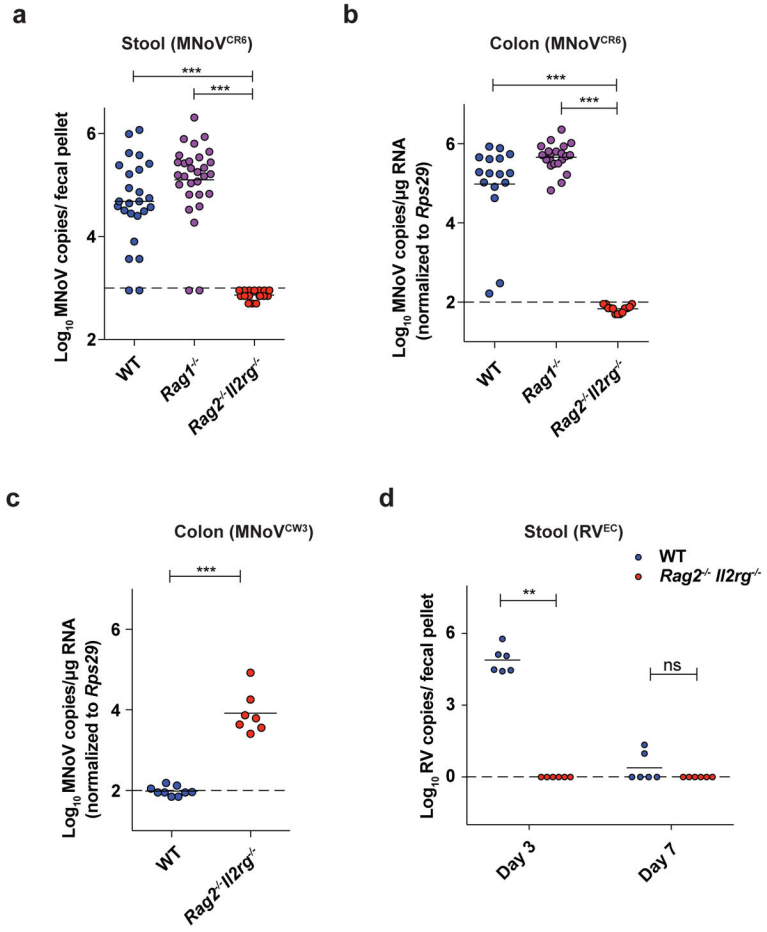

Fig. 1: Specific immunodeficient mouse strains are protected against murine norovirus and rotavirus infection.

(a) MNoV genome copies detected in fecal pellets at 14 days post infection (dpi) in C57Bl/6J wild-type (WT; n=25), *Rag1*$^{-/-}$ (n=28) and *Rag2*$^{-/-}$*Il2rg*$^{-/-}$ (n=17) mice orally infected with 10^6 pfu of MNoV^{CR6}. **(b)** MNoV genome copies detected in colons at 14 dpi in WT (n=16), *Rag1*$^{-/-}$ (n=21) and *Rag2*$^{-/-}$*Il2rg*$^{-/-}$ (n=12) orally infected with 10^6 pfu of MNoV^{CR6}. **(c)** MNoV genome copies detected in colons at 14 dpi in WT (n=9) and *Rag2*$^{-/-}$*Il2rg*$^{-/-}$ (n=7) orally infected with 10^6 pfu of MNoV^{CW3}. **(d)** RV^{EC} genome copies detected in fecal pellets of WT (n=6) and *Rag2*$^{-/-}$*Il2rg*$^{-/-}$ (n=6) mice orally infected with 10^5 SD50 for the indicated timepoints. Results were analyzed by Kruskal-Wallis test followed by Dunn's multiple comparisons test (**a-b**) and Mann-Whitney test (**c-d**) combined from two **(d)** or three independent experiments (**a-c**). *** P =0.0002 **(a)**, *** P <0.0001 (**b-c**), **P=0.0022 **(d)**, ns=not significant **(d)**. Bars indicate mean of all data points.

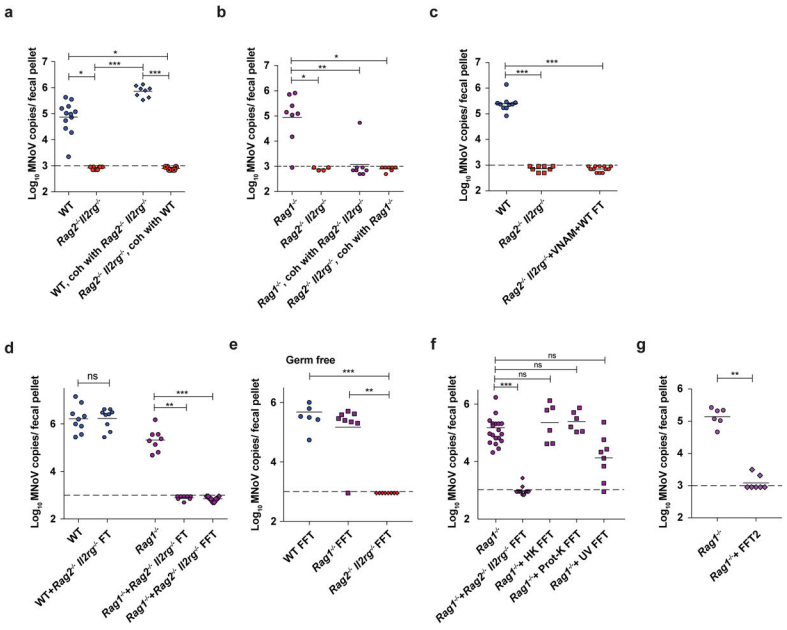

Fig. 2: Antiviral protection is transmissible to immunodeficient, but not immunocompetent mice.

(a-b) Stool MNoV genomes at (**a**) 7 dpi of WT (n=12) or *Rag2*$^{-/-}$*Il2rg*$^{-/-}$ (n=9) controls or WT (n=8) or *Rag2*$^{-/-}$*Il2rg*$^{-/-}$ (n=12) cohoused (coh) for 7 days prior to MNoV^{CR6} infection or **(b)** *Rag1*$^{-/-}$ (n=8) or *Rag2*$^{-/-}$*Il2rg*$^{-/-}$ (n=4) controls or *Rag1*$^{-/-}$ (n=8) or *Rag2*$^{-/-}$*Il2rg*$^{-/-}$ (n=8) cohoused prior to infection. Results from three experiments. For **a**, *P=0.0288 (WT vs *Rag2*$^{-/-}$*Il2rg*$^{-/-}$), *P=0.0156 (WT vs *Rag2*$^{-/-}$*Il2rg*$^{-/-}$, coh with WT), ***P=0.0001. For **b**, *P=0.0288 (*Rag1*$^{-/-}$ vs *Rag2*$^{-/-}$*Il2rg*$^{-/-}$), *P=0.0156 (*Rag1*$^{-/-}$ vs *Rag2*$^{-/-}$*Il2rg*$^{-/-}$, coh with *Rag1*$^{-/-}$), **P=0.0013. **(c)** Stool MNoV genomes at 7 dpi of WT (n=10) and *Rag2*$^{-/-}$*Il2rg*$^{-/-}$ (n=8) mice with no treatment, and *Rag2*$^{-/-}$*Il2rg*$^{-/-}$ (n=12) mice with 14 days of VNAM followed by FT from untreated WT mice 7 days before MNoV^{CR6} infection. Results from two experiments. ***P=0.0007. Results from **a-c** analyzed by Kruskal-Wallis test followed by Dunn's multiple comparisons test. **(d)** MNoV genomes in 7 dpi fecal pellets of WT mice treated with (n=9) or without FT (n=9) from *Rag2*$^{-/-}$*Il2rg*$^{-/-}$ mice 7 days prior to MNoV^{CR6} infection or *Rag1*$^{-/-}$ mice treated with (n=8) or without FT (n=8) or FFT (n=12) from *Rag2*$^{-/-}$*Il2rg*$^{-/-}$ mice 7 days prior to infection. Results from three experiments analyzed using Kruskal-Wallis test and Mann-Whitney test. **P=0.0037, ***P=0.0002. **(e)** Stool MNoV genomes at 7 dpi of germ-free mice treated with FFT from WT (n=6), *Rag1*$^{-/-}$ (n=8) and *Rag2*$^{-/-}$*Il2rg*$^{-/-}$ (n=8) mice for 7 days prior to infection. Results from two independent experiments. **P=0.0014, ***P=0.0004. **(f)** Stool MNoV genomes at 7 dpi of *Rag1*$^{-/-}$ mice untreated (n=19) or treated with FFT (n=13), or FFT heat-killed (HK FFT) (n=6), proteinase K-digested (Prot-K FFT) (n=6) or UV-inactivated (UV FFT) (n=8) for 7 days before MNoV^{CR6} infection. Results from two experiments. ***P=0.0003, ns=not significant. Results from **e,f** were analyzed by Kruskal-Wallis test followed by Dunn's multiple comparisons test. **(g)** Stool MNoV genomes at 7 dpi of *Rag1*$^{-/-}$ mice treated with (n=7) or without (n=6) secondary FFT (FFT2) from *Rag1*$^{-/-}$ mice treated with FFT from *Rag2*$^{-/-}$*Il2rg*$^{-/-}$ for 7 days prior to MNoV^{CR6} infection. Results analyzed by Mann-Whitney test from two experiments. **P=0.0012. Bars indicate mean of all data points.

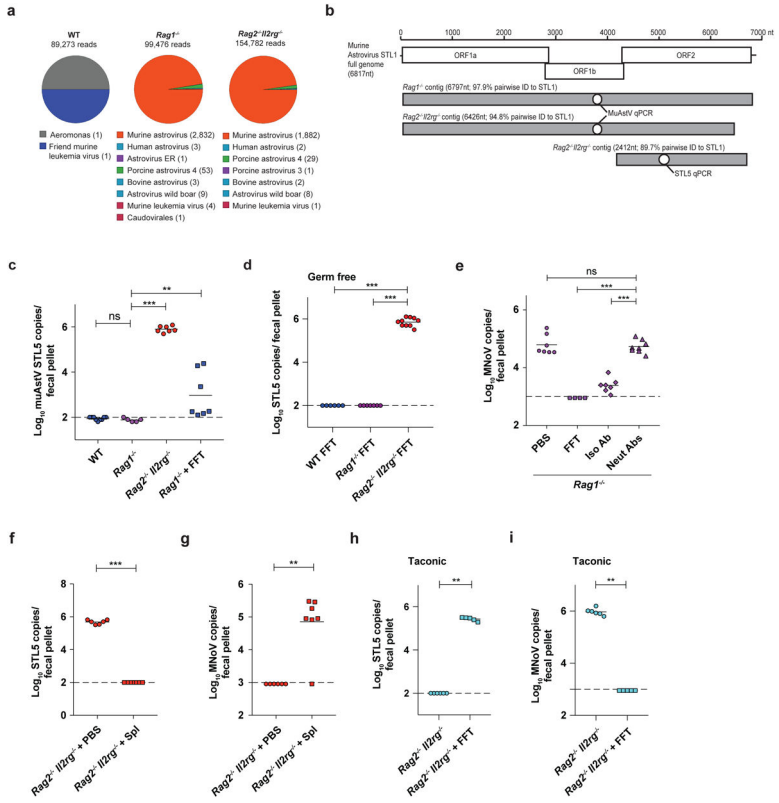

Fig. 3: Murine astrovirus STL5 confers protection against murine norovirus infection.

(a) Pie charts showing the relative abundance of RNA viruses in the FFT material from different mouse strains. Total number of reads analyzed is shown below each genotype; viral assignments are shown with the number of reads assigned per virus in parentheses. **(b)** Alignment of full-length contigs in FFT material from *Rag1*$^{-/-}$ and *Rag2*$^{-/-}$*Il2rg*$^{-/-}$ mice to the STL1 genome. **(c)** Stool STL5 genome copies for WT (n=8), *Rag1*$^{-/-}$ (n=6) and *Rag2*$^{-/-}$*Il2rg*$^{-/-}$ (n=7) mice and *Rag1*$^{-/-}$ (n=7) mice treated with FFT for 7 days. Results analyzed using Kruskal-Wallis test followed by Dunn's multiple comparisons test and Mann-Whitney test combined from three experiments. **P=0.0025 and ***P=0.0002. **(d)** Stool STL5 genome copies for germ-free mice treated with FFT from WT (n=6), *Rag1*$^{-/-}$ (n=7) and *Rag2*$^{-/-}$*Il2rg*$^{-/-}$ (n=10) mice for 5 days. Results from two experiments analyzed using Kruskal-Wallis test followed by Dunn's multiple comparisons test. ***P=0.0003. **(e)** Stool MNoV genomes at 7dpi of *Rag1*$^{-/-}$ mice treated with PBS (n=7) or *Rag2*$^{-/-}$*Il2rg*$^{-/-}$ FFT (n=4) or FFT incubated with isotype IgG (n=7) or mixture of anti-muAstV antibodies (n=8) for 7 days prior to MNoV^{CR6} infection. Results from two experiments analyzed by Kruskal-Wallis test followed by Dunn's multiple comparisons test. ***P=0.0003. **(f)** STL5 genome copies in fecal pellets of *Rag2*$^{-/-}$*Il2rg*$^{-/-}$ mice transplanted with PBS (n=6) or splenocytes (n=7) from FFT-primed WT mice for 14 days. Results from two experiments analyzed by Mann-Whitney test. ***P=0.0002. **(g)** Stool MNoV genomes at 7dpi of *Rag2*$^{-/-}$*Il2rg*$^{-/-}$ mice transplanted with PBS (n=6) or splenocytes (n=7) from FFT-primed WT mice for 14 days. Results from two experiments analyzed by Mann-Whitney test. **P=0.0017. **(h)** Stool STL5 copies in Taconic *Rag2*$^{-/-}$*Il2rg*$^{-/-}$ mice treated with (n=5) or without (n=5) FFT from WashU *Rag2*$^{-/-}$*Il2rg*$^{-/-}$ mice for 7 days. Results from two

experiments analyzed by Mann-Whitney test. **P=0.0022. **(i)** Stool MNoV genomes at 7 dpi of Taconic *Rag2*$^{-/-}$*Il2rg*$^{-/-}$ mice treated with (n=5) or without (n=5) FFT from WashU *Rag2*$^{-/-}$*Il2rg*$^{-/-}$ mice for 7 days. Results from two experiments analyzed by Mann-Whitney test. **P=0.0043, ns=not significant. Bars indicate mean of all data points.

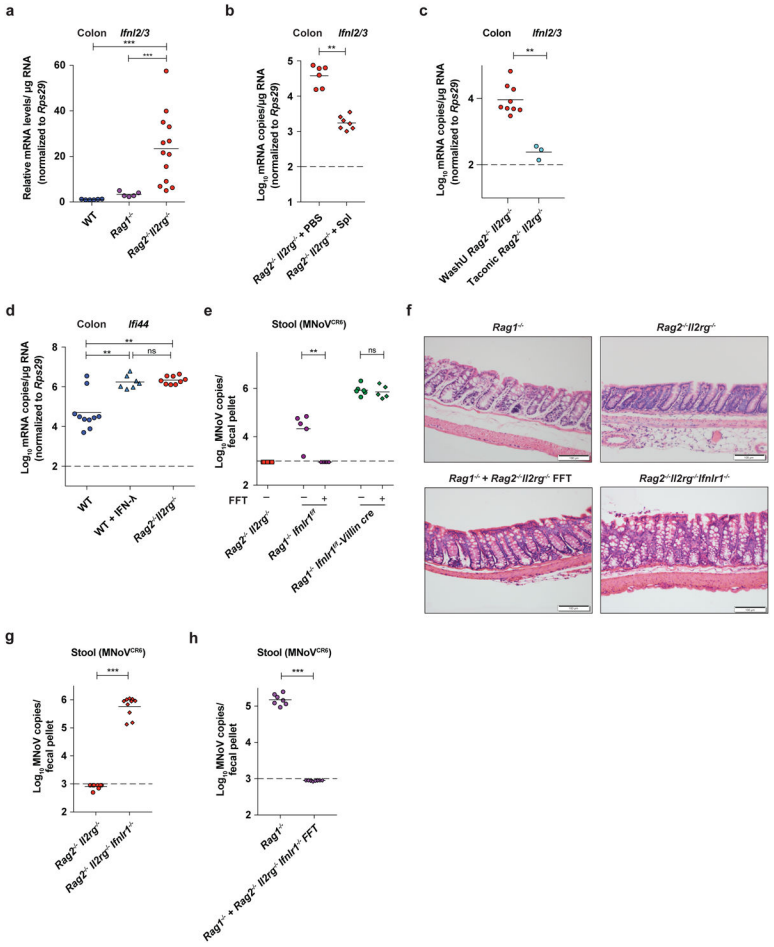

Fig. 4: Intestinal IFN-λ signaling is essential for protection against MNoV in immunocompromised mice.

(a) *Ifnl2/3* mRNA expression in colons of naïve WT (n=6), *Rag1*$^{-/-}$ (n=6) and *Rag2*$^{-/-}$*Il2rg*$^{-/-}$(n=13) mice. Results were analyzed using Kruskal-Wallis test followed by Dunn's multiple comparisons test combined from three independent experiments. ***P=0.0003. **(b)** *Ifnl2/3* mRNA expression in 7 dpi colon of *Rag2*$^{-/-}$*Il2rg*$^{-/-}$ mice transplanted with PBS (n=6) or splenocytes (n=7) from FFT-primed WT mice for 14 days prior to MNoV^{CR6} infection. Results were analyzed using Mann-Whitney test combined from two independent experiments. **P=0.0069. **(c)** *Ifnl2/3* mRNA expression in naive colon of *Rag2*$^{-/-}$*Il2rg*$^{-/-}$ mice from WashU (n=9) or Taconic (n=3). Results were analyzed using Mann-Whitney test one-two independent experiments. **P=0.0091. **(d)** Expression of *Ifi44* mRNA in colons of *Rag2*$^{-/-}$*Il2rg*$^{-/-}$ (n=9), WT (n=10) and WT mice treated with 3µg of IFN-λ (n=7) for 24 hours. Results were analyzed using Mann-Whitney test combined from three independent experiments. **P=0.0089. **(e)** MNoV genome copies detected in 7dpi fecal pellets of *Rag2*$^{-/-}$*Il2rg*$^{-/-}$ mice (n=4), and *Rag1*$^{-/-}$*Ifnlr1*$^{f/f}$ (n=6) or *Rag1*$^{-/-}$*Ifnlr1*$^{f/f}$-*Villincre* mice (n=6) with or without FFT from *Rag2*$^{-/-}$*Il2rg*$^{-/-}$ mice for 7 days before MNoV^{CR6} infection. Results were analyzed using Mann-Whitney test combined from two to three independent experiments. **P=0.0079. **(f)** Representative H&E staining of colon sections from naïve *Rag1*$^{-/-}$ (n=3), *Rag2*$^{-/-}$*Il2rg*$^{-/-}$ (n=3), *Rag1*$^{-/-}$ mice treated with FFT (n=3) from

Rag2$^{-/-}$*Il2rg*$^{-/-}$ mice for 7 days or naïve *Rag2*$^{-/-}$*Il2rg*$^{-/-}$*Ifnlr1*$^{-/-}$ mice (n=3). **(g)** MNoV genome copies detected from 7 dpi fecal pellets of *Rag2*$^{-/-}$*Il2rg*$^{-/-}$ (n=8) and *Rag2*$^{-/-}$*Il2rg*$^{-/-}$*Ifnlr1*$^{-/-}$ (n=8). Results, combined from two independent experiments, were analyzed by Mann-Whitney test. ***P<0.0001 **(h)** MNoV genome copies detected in 7 dpi fecal pellets of *Rag1*$^{-/-}$ mice treated with (n=8) or without FFT (n=7) from *Rag2*$^{-/-}$*Il2rg*$^{-/-}$*Ifnlr1*$^{-/-}$ mice for 7 days before MNoV^{CR6} infection. Results were analyzed using Mann-Whitney test combined from two independent experiments. ***P<0.0001. ns=not significant. Bars indicate mean of all data points.